

Damage-Inducible Intragenic Demethylation of the Human *TP53* Tumor Suppressor Gene Is Associated With Transcription From an Alternative Intronic Promoter

James Blackburn,^{1,2} Daniel L. Roden,³ Robert Ng,^{1,2} Jianmin Wu,^{4,†} Alexis Bosman,⁵ and Richard J. Epstein^{1,2,6*}

¹Laboratory of Genome Evolution, The Kinghorn Cancer Centre, Garvan Institute for Medical Research, Sydney, Australia

²UNSW Medicine, St. Vincent's Clinical School, Darlinghurst, Sydney, Australia

³Laboratory of Cancer Biology, The Kinghorn Cancer Centre, Garvan Institute for Medical Research, Sydney, Australia

⁴Laboratory of Cancer Bioinformatics, The Kinghorn Cancer Centre, Garvan Institute for Medical Research, Sydney, Australia

⁵Laboratory of Developmental and Stem Cell Biology, Victor Chang Cardiac Research Institute, Sydney, Australia

⁶Clinical Informatics & Research Centre, Department of Oncology, St. Vincent's Hospital, Sydney, Australia

Wild-type *TP53* exons 5–8 contain CpG dinucleotides that are prone to methylation-dependent mutation during carcinogenesis, but the regulatory effects of methylation affecting these CpG sites are unclear. To clarify this, we first assessed site-specific *TP53* CpG methylation in normal and transformed cells. Both DNA damage and cell ageing were associated with site-specific CpG demethylation in exon 5 accompanied by induction of a truncated *TP53* isoform regulated by an adjacent intronic promoter (P2). We then synthesized novel synonymous *TP53* alleles with divergent CpG content but stable encodement of the wild-type polypeptide. Expression of CpG-enriched *TP53* constructs selectively reduced production of the full-length transcript (P1), consistent with a causal relationship between intragenic demethylation and transcription. 450K methylation comparison of normal (*TP53*-wildtype) and cancerous (*TP53*-mutant) human cells and tissues revealed focal cancer-associated declines in CpG methylation near the P1 transcription start site, accompanied by rises near the alternate exon 5 start site. These data confirm that site-specific changes of intragenic *TP53* CpG methylation are extrinsically inducible, and suggest that human cancer progression is mediated in part by dysregulation of damage-inducible intragenic CpG demethylation that alters *TP53* P1/P2 isoform expression.

© 2015 The Authors. *Molecular Carcinogenesis* Published by Wiley Periodicals, Inc.

Key words: *TP53*; tumor suppressor gene; cancer; DNA methylation; epigenetics; transcriptional regulation

INTRODUCTION

The *TP53* tumor suppressor gene encodes a tetrameric DNA-binding protein that regulates cell-cycle progression and apoptosis [1]. Unlike many other regulatory genes [2], *TP53* does not contain a 5' CpG island [3] and hence is not transcriptionally repressed by promoter (P1) methylation [4]. However, the gene does contain multiple CpG sites in exons 5–8 which encode the critical DNA-binding domain [5]. Intragenic methylation of these sites can predispose to CG→TA mutations via methylcytosine deamination, a process implicated in human carcinogenesis [6] via either gain- or loss-of-function events secondary to missense or nonsense *TP53* mutations, respectively [7]. Similar mutations occur in response to DNA damage in utero [8], hinting at an adaptive evolutionary explanation for the stringent conservation of these mutation-prone sites [9]. Additional mechanisms implicated in the regulation of p53 function include *hDM2* amplification [10], *ARF* methylation [11], *TP53* alternative splicing [12], microRNA expression [13], and antisense *WRAP53* transcription from the 5' untranslated region of *TP53* [14].

Recent interest has focused on possible function-modifying effects of *TP53* isoforms ($\Delta 133/160$) transactivated by an alternative internal promoter (P2) in intron 4 proximal to codon 40 [12,15,16] (Figure 1). In vitro studies have suggested an inhibitory effect on wildtype p53 of these N-terminal-truncated protein isoforms that lack the first two transactivation

Abbreviations: APGI, Australian Pancreatic Genome Initiative; bp, base pairs; DMEM, Dulbecco's modified Eagle's medium; FBS, fetal bovine serum; Gy, gray (unit of radiation); HEF, human embryonic fibroblasts; iPSC, induced pluripotent stem cells; MEF, mouse embryonic fibroblasts; PBS, phosphate buffered saline; PCR, polymerase chain reaction.

[†]Representing the Australian Pancreatic Cancer Genome Initiative; see Supplementary Table S1.

Grant sponsor: Garvan Institute of Medical Research; Grant sponsor: St. Vincent's Clinic/Curran Foundation

*Correspondence to: Clinical Informatics & Research Centre, The Kinghorn Cancer Centre, 370 Victoria St, Darlinghurst, Sydney NSW 2010, Australia.

Received 24 March 2015; Revised 29 October 2015; Accepted 17 November 2015

DOI 10.1002/mc.22441

Published online 16 December 2015 in Wiley Online Library (wileyonlinelibrary.com).

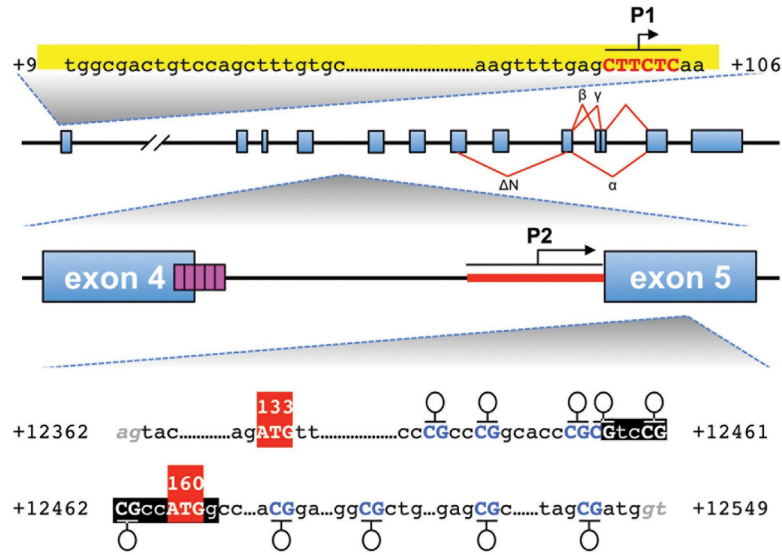


Figure 1. The *TP53* locus with relevant elements expanded and highlighted. Yellow boxed element, proposed mRNA stem-loop structure [51]. Red sequence, major transcription initiation site [51]. Purple boxes, p53 response elements; red line, minimal internal promoter region [20]. Red boxes, ATG start sites. Black box, Kozak consensus sequence [52]. Lollipops, single CpG site. Base numbering from GenBank NC_000017 (7512445..7531642) as per (http://p53.iarc.fr/TP53Sequence_NC_000017-9.aspx).

domains [17]. Consistent with this putative oncogenicity [18], a similar p53 isoform in zebrafish attenuates apoptosis by activating an ortholog of the anti-apoptotic human protein Bcl-x1 [19]. However, despite this apparent anti-apoptotic function, expression of $\Delta 133/160$ isoforms also appears inducible by genotoxic stress [20] through a p53-dependent transactivation mechanism [21], raising the possibility of a negative feedback loop that could be disrupted in pathological states. At a clinical level, expression of $\Delta 133/160$ has been reported in many malignancies, including breast cancer [22], head and neck cancer [23], acute myeloid leukemia [24], melanoma [25], colon cancer [16], and ovarian cancer [26].

Little is agreed, however, as to how the regulation and function of P2-truncated p53 isoforms differs between normal and malignant cells. One plausible mediator of P2 isoform expression is altered intragenic *TP53* methylation. Indeed, dynamic changes of DNA methylation are already known to regulate chromatin structure [27], gene transcription [28] and MeCP2-mediated RNA splicing [29]. The transcribed *TP53* gene body is reported to be widely methylated [30], although it is not known whether such methylation directly facilitates transcription or secondarily reflects enhanced chromatin accessibility to ambient methylases.

The human p53 knock-in (Hupki) mouse is a model system of the *TP53* gene that was constructed via homologous substitution of mouse exons 4–9 with the matching human exons [31,32]. To extend and exploit the latter approach, we have now generated a panel of pre-methylated and non-methylated *TP53* alleles, as well as synonymous CpG-depleted and

-enriched *TP53* alleles, for expression in normal and malignant cell systems. Using a homologous integration method, the present study asks whether changes in intragenic *TP53* methylation are dynamically inducible, whether such changes correlate with altered *TP53* isoform expression, and whether patterns of *TP53* intragenic methylation and/or isoform expression differ between normal and cancer cell systems.

MATERIALS AND METHODS

Mouse Embryonic Fibroblasts (MEFs), Human Embryonic Fibroblasts (HEFs) and Induced Pluripotent Stem Cells (iPSCs), and Mouse Tissues

Cell culture was performed at 37°C in 5% CO₂ within a humidified incubator, and chemicals obtained from Life Technologies, unless otherwise stated. MEF cell suspensions were prepared as described [33]. MEFs were seeded at a density of 5×10^5 cells per 75 cm plate, designated passage 1 (P1), then passaged as per standard 3T3 protocols. For HEF and iPSC production, MEF feeder cells were mitotically inactivated using mitomycin (Sigma-Aldrich, St. Louis, MO), and plated onto 6-well culture dishes (Becton Dickinson, Franklin Lakes, NJ) at a density of 1.25×10^4 cells/cm². Feeder cell culture medium comprised high glucose DMEM, 1× Gluta-max, and 10% FBS. Detroit 551 primary HEFs were obtained from the American Type Culture Collection (ATCC CCL-110). For culture, DMEM was supplemented with 10% heat-inactivated FBS. HEFs were reprogrammed to pluripotency using hSTEMCCA-based lentiviral transfection. iPSCs were cultured and

embryoid bodies prepared as before [34]. Timed pregnant C57/Bl6 females were sacrificed by cervical dislocation at embryonic day 16.5 (E16.5). Embryos were harvested into 1× PBS (Life Technologies, Carlsbad, CA) and tissue biopsied from the limb. Tissue was also biopsied from C57/Bl6 mouse ear, with animals over the age of 8 wk deemed as adult. Cryopreserved viable C57/Bl6 mouse sperm was obtained from Australian BioResources, New South Wales, Australia. All mouse samples were sourced under the Animal Ethics Committee of the St. Vincent's Hospital (Sydney) Campus guidelines.

Human Cancer Cell Culture

The human colorectal adenocarcinoma cell line Caco-2 and the prostate cancer cell line PC-3 were obtained from ATCC (HTB-37 and CRL-1435, respectively). Caco-2 cells do not produce functional p53 due to a truncation mutation in exon 6 [35], although they still produce *TP53* RNA [36]. PC-3 cells also do not produce functional p53 due to a truncation mutation in exon 5 [37].

RNA Extraction, Genomic DNA Extraction, and Bisulfite Treatment

Total RNA was isolated using RNeasy Plus Mini Kit (Qiagen, Valencia, CA). cDNA was prepared from total RNA (QuantiTect Reverse Transcription Kit, Qiagen); ~50 ng was used for qPCR with TaqMan Gene Expression Assays (*P1* (TA/Δ40p53) and *P2* (Δ133p53) [38]; *β-ACTIN* Hs01060665_g1; *Trp53* Mm01731290_g1; *β-actin* Mm01205647_g1) in the presence of TaqMan Gene Expression Master Mix (Life Technologies) using PRISM7900 HT PCR system (Applied Biosystems, Foster City, CA). DNA was extracted from cells and tissues using the QIAGEN DNeasy Blood & Tissue Kit, with the standard protocol. DNA was extracted from mouse sperm using the QIAGEN DNeasy Blood & Tissue Kit and online user-developed protocol. To exclude the possibility of base mutation, the status of *Trp53* exon 5 was assessed by designing primers that span the exon—MusP535Fn, MusP535Rn—as shown in Supplementary Table SII. Primer sequences that amplify *TP53* exon 5 have previously been published; IARC primers P-312 and P-271, http://p53.iarc.fr/download/tp53_directsequencing_iarc.pdf. The mutation status of the *TP53* reconstituted locus was assessed using primers that flank the synthesized insert: forward primers WTF (wildtype), U-nonF (enriched) and U-SF (depleted), and reverse primer GMR. 250–500 ng genomic DNA was bisulfite-treated using the EZ DNA Methylation-Lightening™ Kit (Zymo Research, Orange, CA). Non-methylation-specific PCR primers spanned the coding strand of bisulfite-converted *Trp53* exon 5—MusP535Fbnew, MusP535R2bnew. Primer sequences used for amplification of the coding strand of *TP53* exon 5 were as published (U5_a and U5_b) [32]. The methylation status

of the coding strand alone was assessed, since CpG dinucleotides are symmetrically methylated. Non-methylation-specific PCR primers were also designed to span the coding strand of the bisulfite-converted CpG variable insert—GM_bisF1n, GM_bisRn (Supplementary Table SII).

PCR Subcloning, Sequencing, and Statistical Analysis

PCR products were ligated into pGEM[®]-T Easy Vectors (Promega, Madison, WI) using an insert:vector ratio of 3:1, and colonies selected following screening. Plasmid DNA was isolated using PureYield™ Plasmid Minipreps (Promega). Insert size was determined by *EcoRI* restriction digestion (New England BioLabs, Ipswich, MA). Positive clones were prepared for sequencing using T7 DNA primers, and capillary sequencing performed using a 3130XL Sequencer (Life Technologies, Carlsbad, CA). Pop7 polymer and BigDye3.0 was used, with clean-up by Agilent Cleanseq magnetic beads. For each sample, 16 subclones were randomly sequenced. The methylation status of each CpG site was collated into binary maps (1 = demethylated; 0 = methylated). Each sampling was performed in triplicate. A statistical platform was developed to determine whether differences in the methylation status for each CpG site were significant. For each binary map, the data were randomized 10,000 times, and for each CpG site, the assigned fraction of demethylation was calculated. This assignment was assumed to be a normal distribution. A z-score was calculated to discern where the fraction of demethylation lay on the normal distribution curve. For each CpG site, a 2-sided *P*-value calculation was derived from the z-score to determine whether a given CpG site was methylated or demethylated at a level higher than expected from normal or random distributions.

Reconstitution of Wildtype *TP53* in Caco-2 Cells

The sequence encoding *TP53* exons 5–8 was synthesised (DNA2.0) with two further sequences developed—one synonymously enriched for CpG content, and other synonymously depleted of CpG content (Supplementary Figure S1). These sequences were flanked by 90 bp of introns 4 and 8, capped with restriction sites for *EcoRV* and *BglIII*. PCR primers were designed to span ~900 bp 5' to exon 5 and ~900 bp 3' to exon 8, corresponding to exons 4 and 9, partial intronic flanking sequence and engineered capping restriction sites for *NotI/SpeI* and *BglIII/NotI*—Hu34F, Hu34R (5'); Hu9F, Hu9R (3') (Supplementary Table SII). PCR was performed on 100 ng genomic DNA in a 50 μl reaction for 35 cycles. PCR products were separated on a 1% agarose gel and purified using the Wizard[®] SV Gel and PCR Clean-Up System (Promega). These elements were digested and ligated for construction of pGEM-5Zf(+)-based (Promega) plasmid constructs comprising the synthesized DNA, the flanking sequences, and a selective element

derived from pSEPT plasmid (*SpeI/EcoRV*). The CpG-variable construct (vc-*TP53*) was packaged into recombinant adeno-associated viral particles using AAV-DJ helper-free expression (Cell Biolabs, Inc., San Diego CA) and the HEK293T cell line. The virus produced was used to transduce Caco-2 cells; particle production, transfection, and cell selection was performed as described [39] with 1200 $\mu\text{g ml}^{-1}$ Geneticin (Life Technologies) for Caco-2 cell selection. The polyA sequence 3' to the Neo^R selective element truncates the *TP53* allele, enabling cells to be selected prior to p53 activation through Cre-mediated excision of the selective element (Supplementary Figure S2). pTrip-CMV-nlsCre lentivirus (Dr. Philippe Ravassard, French National Centre for Scientific Research (CNRS), Paris, France) was used to excise the selective element and reconstitute the *TP53* locus. CpG-variable Caco-2 cells were harvested prior to, and 24 h following, *TP53* activation, with the objective of measuring p53 DNA, RNA, and protein content.

X-Irradiation and Western Blotting

Cells were exposed to 2Gy irradiation, using an X-RAD 320 Biologic Irradiator (Precision X-Ray). p53-activated CpG-variable Caco-2 cells were irradiated 24 h following *TP53* activation. For western blotting, cells were lysed using RIPA lysis buffer (20 mM Tris-HCl, 200 mM NaCl, 1 mM EDTA pH 8.0, 0.5% NP-40) supplemented with protease inhibitors (Complete, EDTA-free protease inhibitor cocktail, Roche Diagnostics, Rotkreuz, Switzerland). The following antibodies were used: mouse anti-p53 (DO-1) and mouse anti- β -actin (AC-15), both from Santacruz Biotechnology, CA; and HP-linked sheep anti-mouse (GE Healthcare, UK).

Methylation in Primary and *TP53*-Mutated Cells, and Adjacent Normal Tissue Versus Mutant Tumors

Methylation data from genomic analyses of Illumina Infinium HumanMethylation450 (HM450K) arrays were either accessed from the Australian Pancreatic Cancer Genome Initiative (APGI) patient cohort or downloaded for primary cells and *TP53*-mutated cell-lines (Supplementary Table SIII). Methylation beta-values were downloaded from (www.marmal-aid.org) or GEO (ftp://ftp.ncbi.nlm.nih.gov/geo/series/GSE52nnn/GSE52025/matrix/GSE52025_series_matrix.txt.gz). Probe comparisons and statistics were calculated using Wilcoxon rank-sum statistics.

RESULTS

Site-Specific CpG Demethylation of *TP53* Exon 5 Occurs During Cellular Passaging/Ageing, and Is Also Inducible by X-Irradiation in Non-Cancer Cells

For analysis of mouse tissue, primary mouse embryonic fibroblasts (MEF), and human induced pluripotent stem cells (iPSCs), DNA was extracted,

bisulfite-converted, PCR-amplified, subcloned, and sequenced. Comparison of the methylation profile of primary MEF cells with passage 14 cells revealed a single nonrandom site-specific demethylation event in the multi-passaged cells within exon 5 at residue 4, corresponding to mouse codon R153 (CGT; Figure 2A). Mouse exon 5 contains 11 CpG sites. This pattern of demethylation was not identified in exons 6–8 (data not shown). To assess whether this site-specific change in methylation status also occurs in vivo, we compared the methylation profiles of biopsied E16.5 (limb) and >8-wk old (ear) C57/Bl6 mouse tissues, termed embryonic and adult, respectively. The comparison revealed a similar demethylation pattern in adult tissue with significance at the same residue identified in the MEFs, corresponding to mouse codon R153/CGT; of note, this demethylation event was also detectable in murine sperm (Figure 2B). Comparison of the methylation profile of human day 0 iPSCs (d0) with day 45 cells (d45) also confirmed a single site-specific demethylation event in the multi-passaged cells within exon 5, but at residue 1, corresponding to human codon P152/CCG (Figure 2C). Human exon 5 contains 10 CpG sites. This pattern of demethylation was not identified in exons 6–8 (data not shown). The human demethylation site was 11 bp upstream of that identified in the mouse, although both reside within 14 bp upstream of a Kozak consensus sequence—an evolutionarily conserved eukaryotic sequence implicated in translational initiation. Importantly, demethylation at the above mouse and human CpG sites was inducible in intragenically methylated genes by sublethal X-irradiation (Figure 2A and C: P1 XR/d0 XR).

Exon 5 Demethylation Is Associated With Increased *TP53* Transcription From Both the P1 and P2 Promoters

To assess the potential effects of methylation change on *TP53/Trp53* transcription, we performed qPCR using RNA extracted from passaged primary MEFs and human iPSCs. An increase in gene transcription was observed between initial and passaged cells, both human and murine (Figure 3A and B). *TP53/Trp53* expression was also inducible, although to a marginally lower extent, by sublethal irradiation. Due to the proximity of exon 5 to the alternative internal promoter at the 3' end of intron 4 (P2; Figure 1), we assessed the effects of methylation on P2-derived transcription using qPCR of differentiated human iPSCs. Again, increased gene transcription was observed between the initial and differentiated cells, with this increase also inducible by sublethal irradiation (Figure 3C).

DNA Damage-Inducibile Upregulation of *TP53* Expression From the Internal P2 Promoter Is Not Evident in Cancer Cell Lines

To clarify the effects of methylation on the relative activation of P1 and P2 promoters, we synthesized a

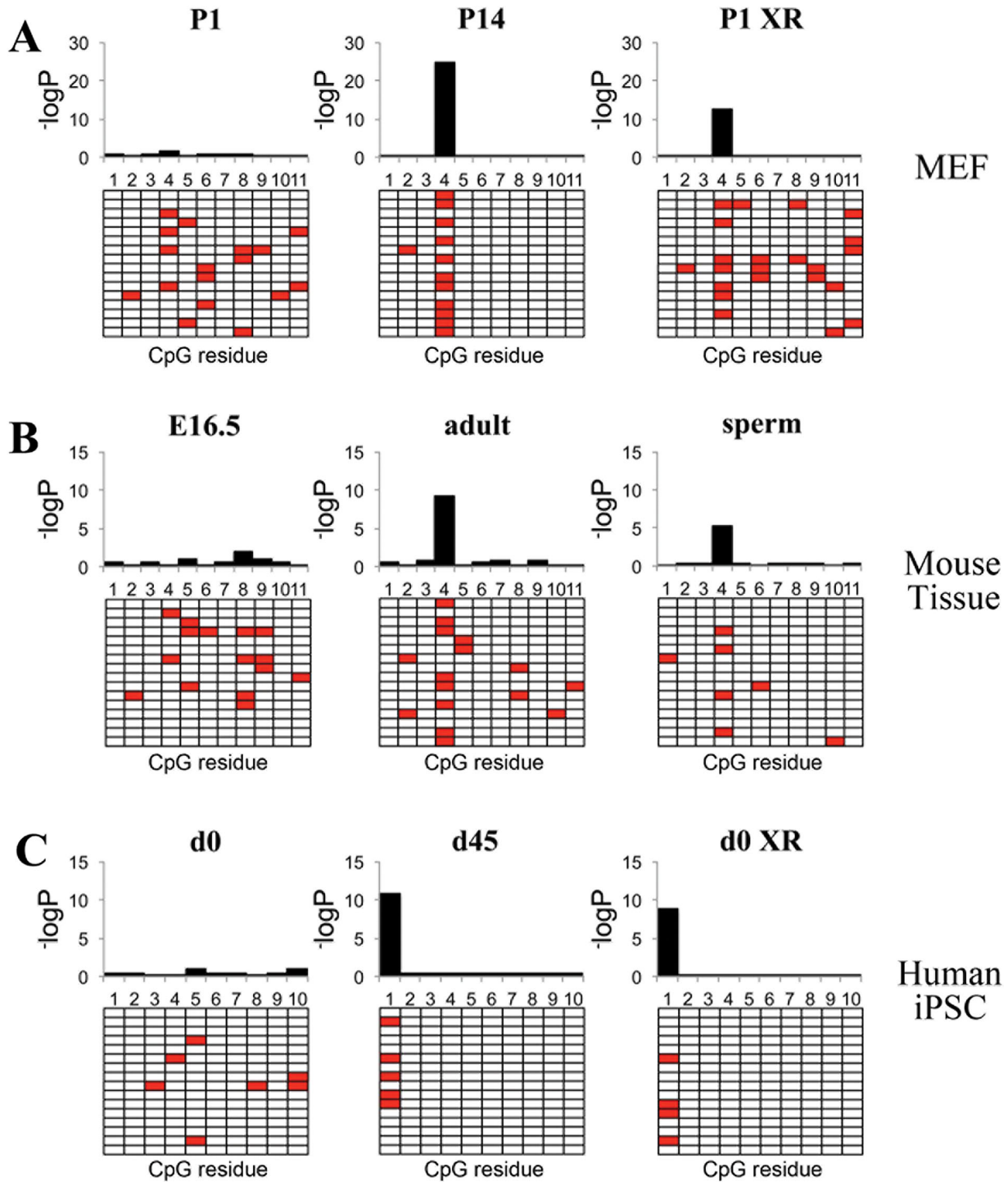


Figure 2. *Trp53* / *TP53* exon 5 CpG methylation analysis. A: MEF cells: passage 1 (P1) and 14 (P14), and X-irradiated P1 (P1 XR). B: Mouse tissues; embryonic day 16.5 (E16.5; limb), adult (>8 wk old; ear), and sperm. C: Human iPSC cells: day 0 (d0) and 45 (d45), and X-irradiated d0 (d0 XR). X-axis = exon 5 CpG residue number (mouse–11; human–10). Y-axis = $-\log_{10}$ of the demethylation statistical *P*-value. Grids represent binary bisulfite maps of an example set of 16 PCR-derived subclones. Red shading represents CpG site demethylation.

TP53 partial cDNA spanning exons 5–8 (encoding amino acids 126–306). This was incorporated into *TP53* null cell lines Caco-2 [35] and PC-3 [37] using virally mediated homologous recombination (see

Materials and Methods section). The integration event repairs the *TP53* locus in these cells, but an internal polyA sequence within the selective element truncates the allele, allowing selection for

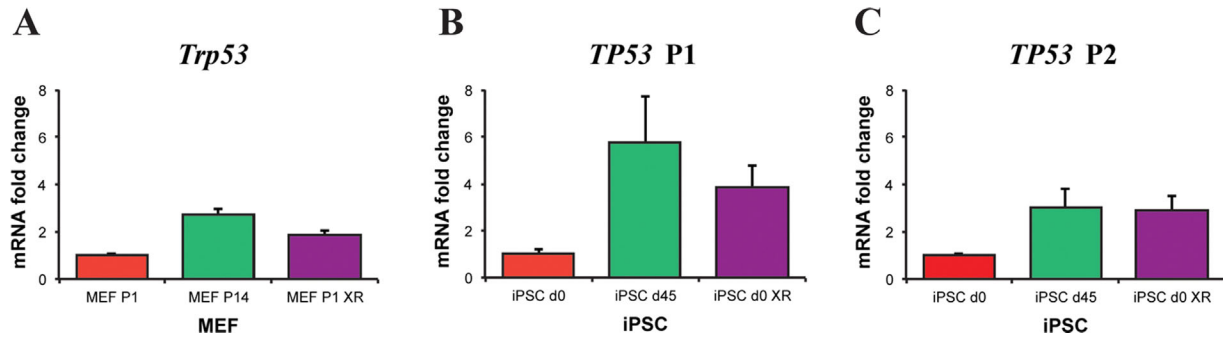


Figure 3. qPCR gene expression data for p53 loci, normalized to β -actin. A: Mouse *Trp53*. B: Human *TP53* from promoter P1. C: Human *TP53* from promoter P2. mRNA fold change is relative to the original cell source (passage 1 MEF; day 0 iPSC) with bars for standard error. MEF, mouse embryonic fibroblast; P1, cell passage 1; P14, cell passage 14; XR, X-irradiated; iPSC, induced pluripotent stem cell; D0, culture day 0; D45, culture day 45.

recombination prior to initializing *TP53* activity. Initial analysis of the methylation profile of exon 5 in the parental cell lines revealed full methylation, that is, complete absence of CpG site demethylation (Figure 4A). Transduced Cre-activated wildtype alleles (see Materials and Methods section) in both the Caco-2 and PC-3 cell lines show increased *TP53* transcription that is further enhanced by sublethal irradiation (Figure 4B). Both observations are corroborated by the presence of p53 protein in lysates from activated and irradiated cells (Figure 4C). Of note, P2-derived transcription is also increased following activation, but sublethal X-irradiation attenuates this in both of these cancer cell lines (Figure 4D).

In Vitro Methylation of *TP53* Reduces Expression From Both P1 and P2 Promoters

To assess the effect of methylation status of *TP53* on gene expression, we created partial cDNAs based on frame-independent dinucleotides and in-frame codons of exons 5–8. These comprised wild-type, CpG-enriched, and CpG-depleted synthetic constructs (Supplementary Figure S1). These constructs were virally integrated into Caco-2 cells (Supplementary Figure S2). Since bacteria do not methylate CpG, the bacterially propagated constructs were methylated in vitro using *SssI* methylase (New England Biolabs) prior to transfection into the viral packaging line. In vitro methylation and activation of wild-type (WT) CpG-containing alleles suppresses *TP53* expression from the P2 promoter, whereas for the CpG-enriched (En) variant, in vitro methylation also suppresses expression from P1. As expected, in vitro methylation of CpG-depleted (De) alleles has no inhibitory effect on expression from either the P1 or P2 promoter, both of which continue to transcribe (Figure 5A). This concurs with *TP53* transcription for all of the alleles in the absence of in vitro methylation (Figure 5B). Following exposure to sublethal irradiation, P1-derived transcripts are elevated in both the methylated and unmethylated formats, excepting the methylated CpG-enriched allele which shows no

change. Conversely, sublethal irradiation attenuates P2 transcription in Caco-2 cells (Figure 5A).

Site-Specific *TP53* Exon 5 CpG Mutation Frequency in Archival Tumors Varies Inversely With Demethylation Frequency of the Same CpG Sites

To assess the relevance of *TP53* exon 5 demethylation to tumor biology, we defined the exonic methylation profile for eight human tumors using the same methodology used earlier to screen the mouse tissue, MEFs, and iPSCs, corrected for orthologous sequence variation (Supplementary Figure S3). Comparison of the cumulative methylation profile of these tumors with the known frequency of CpG-specific somatic mutation in all tumors (<http://p53.iarc.fr/TP53SomaticMutations.aspx>) revealed an inverse association between methylation and mutation frequency, with a Spearman's rank correlation of -0.77 and P -value of 0.005 (Supplementary Table SIV). These data are consistent with the notion that intragenic methylation is associated with reduced transcription-coupled repair of mutations (i.e., implying reduced focal accessibility to repair enzymes) in cancer cells.

The Intragenic Methylation Density of *TP53* Rises Sharply but Variably 3' to Exon 1

To define the intragenic methylation landscape of *TP53*, we first analyzed the topographic methylation profiles of all three genes of the *TP53* superfamily using 66 primary cell Illumina 450K methylation arrays (Supplementary Table SIII). The profile for *TP53* showed hypomethylation of the 5' end of the locus, succeeded by a sharp rise of CpG methylation after the first intron (Supplementary Figure S4A). In contrast, the methylation landscape for *TP63* was variable across the locus with methylation levels remaining high, whereas that of *TP73* exhibited larger oscillations over the course of the gene (Supplementary Figure S4C). Hence, although *TP53* gene family members share an internal alternative promoter sequence [40], the methylation landscape of *TP53*

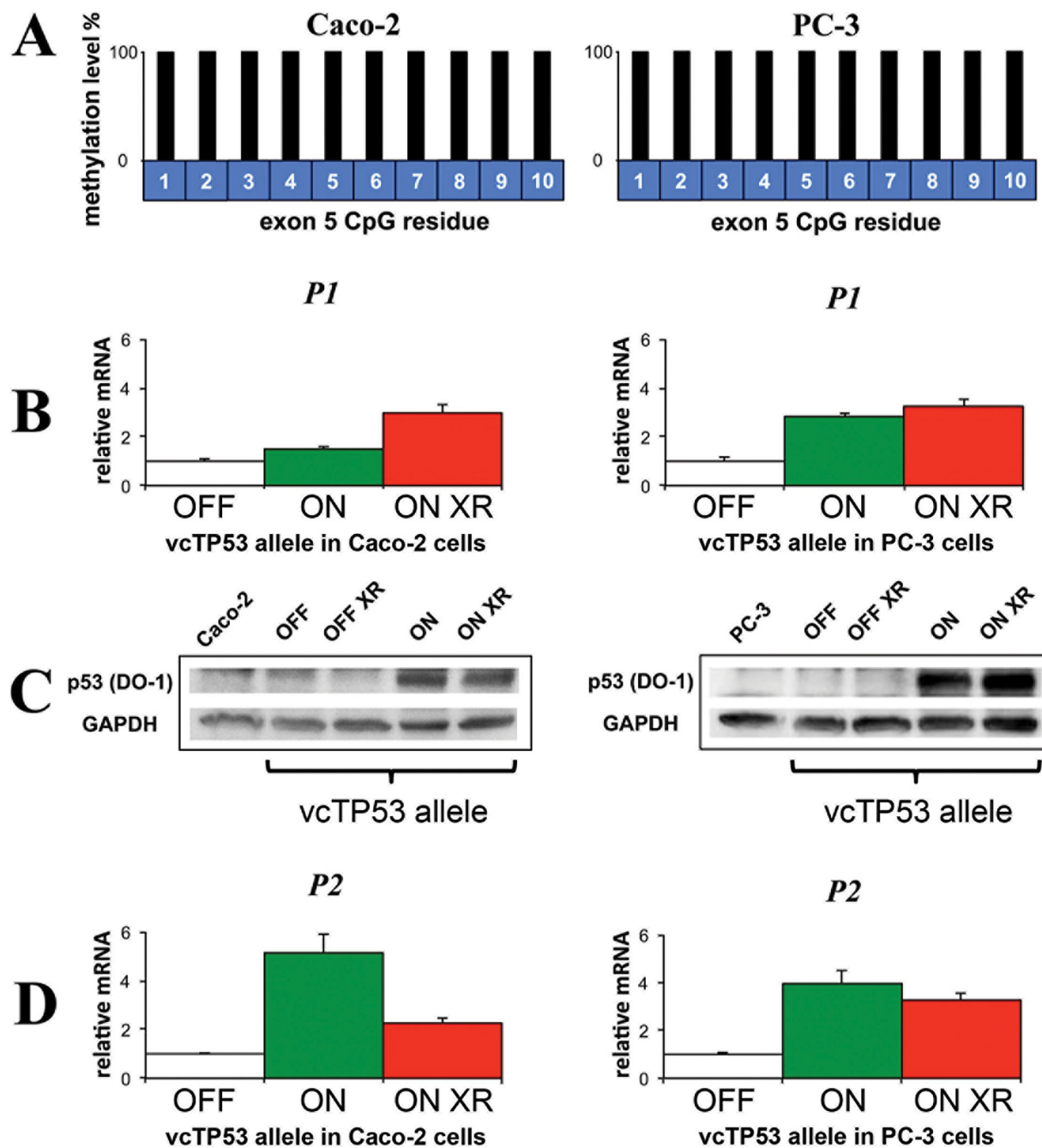


Figure 4. *TP53* methylation status for Caco-2 and PC-3 cell lines, and RNA and protein expression following reconstitution of a functional *TP53* locus. A: Methylation levels of the *TP53* exon 5 CpG residues for Caco-2 and PC-3 parental cell lines. The data in B to D represents the reconstituted *TP53* locus (vcTP53) in two states (OFF and ON) and in two conditions (\pm X-irradiation [XR]). B: qPCR data for fold change of full-length *P1* *TP53* mRNA. C: protein expression data for full-length p53 and GAPDH. D: qPCR data for the fold change of *P2* mRNA isoforms. Data in B and D are normalized to β -actin. Fold change is relative to the original cell source (OFF).

appears distinct, perhaps reflecting a more transcriptionally active role in differentiated adult tissues.

We then sought to determine the methylation landscape of the *TP53* locus in *TP53*-mutated versus -wildtype cell lines by analyzing data from 32 Illumina 450K methylation arrays (Supplementary

Table SIII). As with primary cell analysis, the overall profile was that of low-level methylation status of the 5' end of the locus followed by a sharp rise after intron 1 (Supplementary Figure S4A). However, the methylation value of the probe in the transition region (cg07760161) was higher in primary (*TP53*-wildtype)

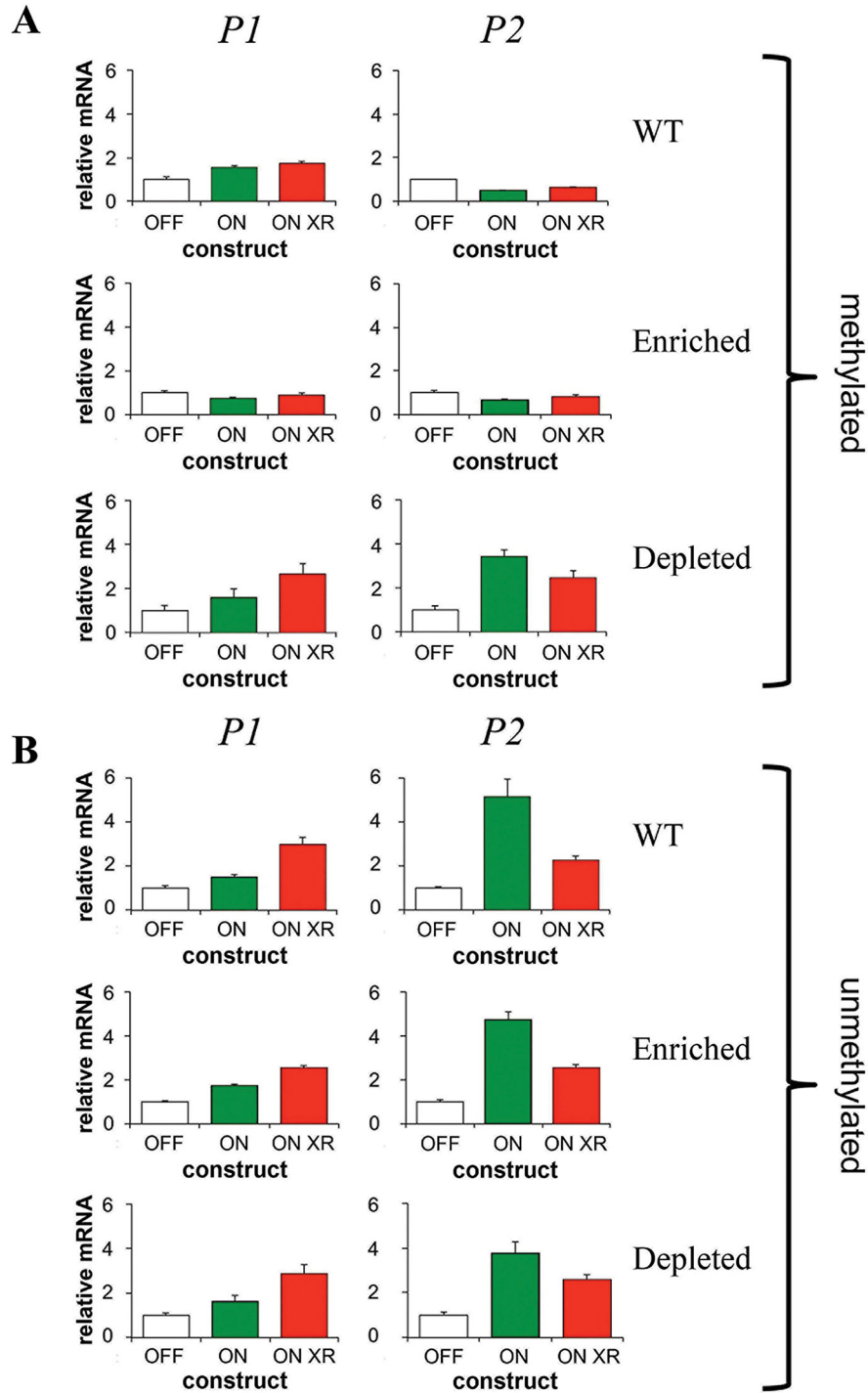


Figure 5. qPCR gene expression data for Caco-2 cells following reconstitution of a functional *TP53* locus, using CpG variable alleles (WT construct; CpG-enriched construct; CpG-depleted construct) with and without in vitro methylation prior to integration, for fold change of full-length *P1 TP53* and *P2* mRNAs. A: Methylated. B: Unmethylated. OFF, construct integrated. ON, construct integrated and activated. ON XR, active construct additionally X-irradiated. Data are normalized to β -actin. Fold change is relative to the original cell source (OFF).

cells compared to the *TP53*-mutant subgroup (Figure 6A, $P = 7.13 \times 10^{-9}$). In addition, the difference in methylation value between the transition region probe and the adjacent (high methylation) probe

(cg12041429) was lower in primary cells (Figure 6B, $P = 2.03 \times 10^{-7}$), indicating higher levels of methylation in this region in primary cells. The methylation landscape of the *TP53* locus was then assessed in a

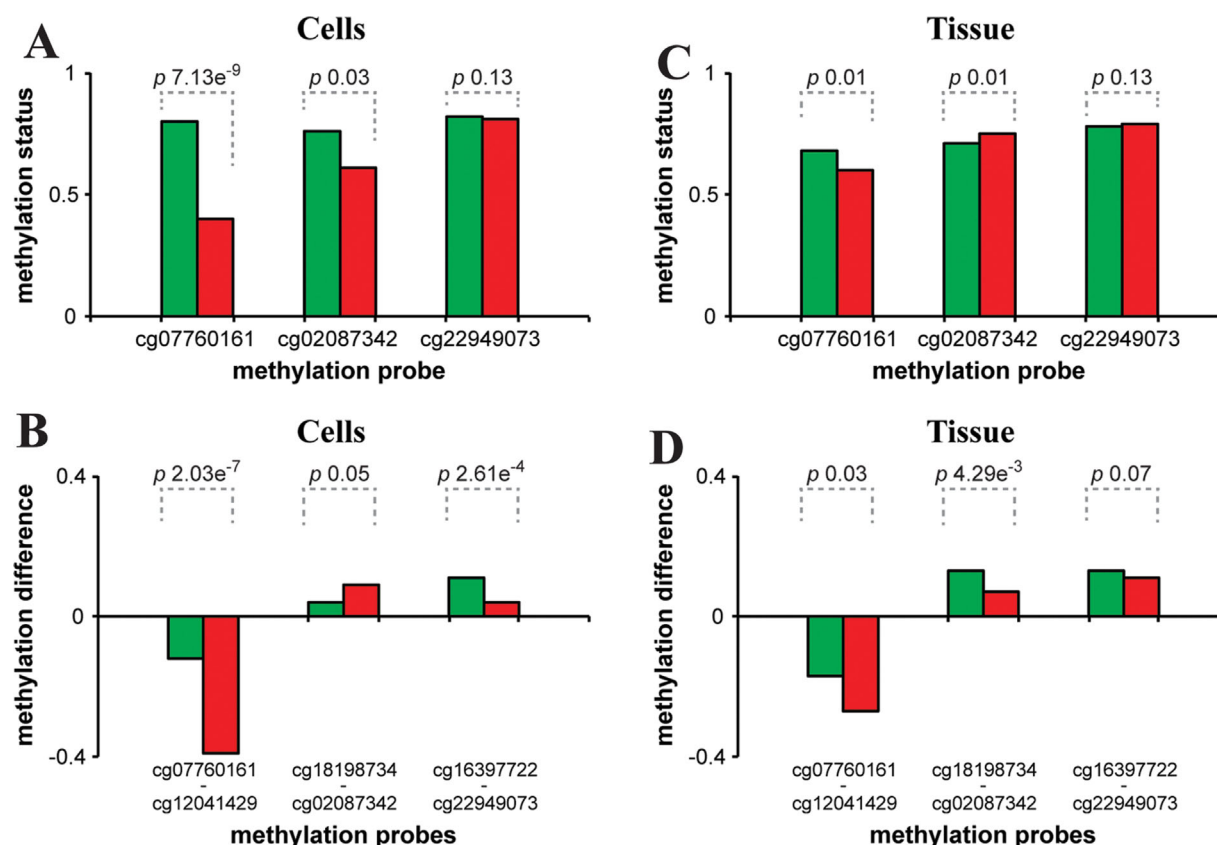


Figure 6. Illumina 450 K methylation array data for *TP53*-mutated tumor biopsies and cell lines. A and B: Primary cells compared to *TP53* mutant cell lines. C and D: APGI patient cohort tumor samples compared to adjacent normal tissue. Green, primary cell or normal adjacent tissue. Red, *TP53* mutant cell or tumor biopsy. A and C: Median β -values of methylation for single probes in regions of methylation transition. B and D: subtractive differences in methylation of adjacent probes (probe 1–probe 2) in regions of methylation transition. *P*-values displayed assess the differences between the subgroups and were calculated using the Wilcoxon rank sum test.

cohort of human pancreatic tumors using Illumina 450 K methylation array data from the APGI database. We compared the methylation profile of 24 adjacent normal tissues with 64 *TP53* mutant tumors (Supplementary Figure S4B). Again, higher methylation is evident in the transition region in normal tissues compared to tumors (Figure 6C, $P = 0.01$). Following the rapid rise in *TP53* locus methylation, there is a decrease in methylation followed by a secondary rise in all four subgroups (Supplementary Figure S4A and B, bottom panel). The value of the probe at the base of the methylation dip (cg02087342) differs between both the primary cells versus the *TP53*-mutant cells, and the normal tissues versus *TP53*-mutant tumors (Figure 6A and C, $P = 0.03$ and 0.01 , respectively). The difference between the methylation dip probe and the 5' adjacent probe (cg18198734) likewise differs between these subgroups (Figure 6B and D, $P = 0.05$ and 4.29×10^{-3} , respectively). These reproducible mutation-associated variations in *TP53* methylation patterns are again consistent with a functional significance—whether direct or secondary—for focal intragenic demethylation events.

Intragenic 450 K Methylation Profiles may Vary Between Functionally Distinct Gene Classes

To gain insight into the significance of the *TP53* intragenic methylation pattern, we then examined the 450 K methylation profiles of genes from different functional classes—housekeeping genes, oncogenes, gatekeeper suppressor genes, caretaker suppressor genes, and tissue-specific (i.e., differentiation-specific) genes—for which differences in expression levels in normal primary (epithelial) cells would be reasonably expected. To this end we analyzed data from 66 primary cell Illumina 450 K methylation arrays for genes with at least 10 CpG probes covering the loci. The following genes were selected as examples of the above functional groups: *TUBB* (housekeeping gene encoding β -tubulin); *MYC* (proto-oncogene); *PTEN* (gatekeeper suppressor gene); *ATM* (caretaker suppressor gene); and *CNP* (a neuron-specific gene encoding 2',3'-cyclic-nucleotide 3'-phosphodiesterase, which should not be expressed in epithelial cells). All these genes possess 5' promoter CpG islands (Supplementary Table SV). In terms of

their 450K profiles in normal cells, all exhibit some degree of 5' hypomethylation; the extent to which this was maintained along the 3' course of the gene seemed to vary broadly in the order of expected transcriptional activity, with the housekeeping gene and proto-oncogene remaining most hypomethylated, the neuron-specific gene least, and the tumor suppressor genes intermediate (Supplementary Figure S5). Although not conclusive proof, these data are consistent with a causal link between intragenic demethylation and gene functionality.

DISCUSSION

The central finding of this study is that dynamic site-specific alterations of intragenic gene methylation are associated with hitherto unreported functional effects. Specific observations supporting this conclusion are that (i) CpG-specific intragenic *TP53* demethylation occurs following DNA damage induction or accumulation in non-cancer cells and tissues, though evidently less so in cancer cells and tumors; (ii) unique demethylation events affecting intron 4/exon 5 appear spatially and temporally associated with transcription from the P2 internal promoter regulating the 5'-truncated *TP53* ($\Delta 133/160$) isoform; and (iii) the intragenic methylation status of *TP53* and its paralogs (*TP63*, *TP73*) varies widely across the intron/exon landscape of these and other genes.

In agreement with earlier studies into the human and Hupki genomes [30,41], our results confirm that most of the *TP53* gene—notably the genomic sequence 3' to intron 1—is indeed predominantly methylated, notwithstanding our finding of site-specific demethylation. The latter discrepancy reflects the fact that the observed demethylation events are incomplete, with far more methylation remaining detectable (e.g., in the relevant regions of intron 4/exon 5) than in gene regions proximal to intron 1 (Supplementary Figure S4A). This raises the possibilities that either (i) only partial demethylation is occurring, or else (ii) full site-specific *TP53* demethylation, if it occurs, is restricted to a subset of cells at any one time. Both of these possibilities are consistent with the proposal by Jjingo et al. that any positive correlation between total intragenic methylation and transcriptional activity could arise secondary to increased chromatin accessibility in active genes, which by default increases gene body accessibility to other proteins such as methylases. In other words, gene body methylation may not directly effect transcriptional activation, but could rather be a biomarker of open chromatin conformation [42]. A corollary of this hypothesis is that intragenic DNA demethylation may arise not through demethylase activity per se, but via competitive binding of non-methylase or non-methyl-binding proteins such as trans-acting factors, repair enzymes or chromatin proteins [43]. Our data also support the conclusion of Shenker and Flanagan that hypomethylation

characterizes the 5' region of highly expressed genes not only the promoter region, as seen in genes with 5' CpG islands, but also the first exon and intron [44] (Supplementary Figure S4A), as might be consistent with a regional change in chromatin conformation.

That the correlation of internal P2 *TP53* promoter utilization (Figures 3 and 4) and focal demethylation (Supplementary Figure S4; Figure 6) is likely causal is supported by our experiments using custom-designed methylated versus unmethylated *TP53* exonic constructs of divergent CpG content (*vcTP53*; Figure 5). Against this, we note the view of Bauer et al. that CpG depletion is associated with reduced transcription [45], implying a direct transcription-promoting effect of methylation. However, these experiments were based on CpG content alone rather than on methylation status per se. Our *vcTP53* experiments directly address this issue for the first time, and are supported by the data in Supplementary Table SIV confirming an inverse correlation between CpG site-specific *TP53* exon 5 mutation and demethylation frequencies in human tumors. Pogribny et al. reported that DNA damage can trigger DNA demethylation by reducing expression of post-replication maintenance methylases such as DNMT1 [46], consistent with our finding of radiation-induced focal demethylation (Figures 2–6). Moreover, both Kulis et al. and Maunakea et al. reported that reductions in intragenic methylation can activate internal promoter usage [47,48]. This possibility is consistent with recent work quantitatively associating intragenic methylation of the *ATM* tumor suppressor gene with breast cancer risk [49].

There remain several important limitations of this study, however. First, our observation of localized intragenic demethylation falls short of establishing a molecular explanation for the association with alternate promoter usage—such as may require methylation footprinting studies or single-cell epigenomics—nor does our work shed light on the known correlation between global DNA hypomethylation and tumorigenesis [50]. Second, the specific site-specific demethylation events seen in the mouse and human genes (Figure 2) do not match exactly in terms of location, and the significance if any of this difference is unknown. Third, our variably methylated alleles (Figures 4 and 5) likewise do not match the single site-specific location of the demethylation event detected in Figure 2, but rather exaggerate this. Fourth, our work does not establish a biological role for the observed aberrant methylation of *TP53* introns 1 and 4. However, since no common mutational events affect these introns in tumors, the possibility of hitherto unrecognized epigenetic modifications contributing to cancer progression remains intriguing. Fifth, the study has not defined a detailed molecular mechanism to explain the relationship between the observed intragenic demethylation events and P2 induction.

However, another unexplained aspect of this work concerns the functional significance of the *TP53* P2 Δ 133/160 isoform in tumor cells. Other groups have implicated this isoform as having an anti-apoptotic *TP53*-inhibitory function [17,19]; to our surprise, the present study showed a decline in damage-inducible P2 transcript production relative to controls in virally transduced human cancer cell lines of parental *TP53*-mutant p53-null genetics (Figures 4 and 5), which is the opposite trend to that seen in *TP53*-wildtype cell lines (Figure 3C). Preliminary experiments had suggested that expression of the p21-encoding *CDKN1A* gene parallels P2 rather than P1 *TP53* transcript expression in these cancer cell lines (unpublished data). Perhaps consistent with this, a study in leukemia patients reported that chemotherapy damage repressed expression of the Δ 133/160 P2 isoform while upregulating expression of the wild-type p53 protein [24], suggesting a novel pathway contributing to drug resistance acquired by *TP53*-defective tumors during cytotoxic treatments. More work is needed to clarify the complex genetic and signaling interactions that may underlie the experimental observations of this study.

In conclusion, the present study suggests a novel dimension of *TP53* gene regulation involving topographically localized intragenic demethylation events that could modulate internal promoter usage. Future studies are needed to define the molecular physiology underlying these observations, and hence to design clinically applicable drug strategies for overcoming *TP53*-dependent cell resistance and genetic instability in cancer patients.

ACKNOWLEDGMENTS

We thank Prof. Andrew Biankin and Prof. Sean Grimmond for access to 450K methylation data of the APGI patient cohort; Prof. Richard Harvey for help from the Developmental and Stem Cell Biology Laboratory, Victor Chang Research Institute; Dr. Alex Swarbrick for access to Victorian Cancer Biobank DNA; A/Prof. Maija Kohonen-Corish for access to colon cancer cohort DNA; Dr. Akira Nguyen for generating the MEFs; Dr. Atsushi Ohazama for provision of embryonic mouse tissue; Kevin Taylor from Australian BioResources (NSW) for providing mouse sperm; and Prof. Allan Spigelman and the St. Vincent's Cancer Programme for infrastructural support.

REFERENCES

- Lane D, Levine A. P53 research: The past thirty years and the next thirty years. *Cold Spring Harb Perspect Biol* 2010;2:a000893.
- Esteller M. Epigenetic lesions causing genetic lesions in human cancer: Promoter hypermethylation of DNA repair genes. *Eur J Cancer* 2000;36:2294–2300.
- Bienz-Tadmor B, Zakut-Houri R, Libresco S, Givol D, Oren M. The 5' region of the p53 gene: Evolutionary conservation and evidence for a negative regulatory element. *EMBO J* 1985;4:3209–3213.
- Barekati Z, Radpour R, Kohler C, et al. Methylation profile of *TP53* regulatory pathway and mtDNA alterations in breast cancer patients lacking *TP53* mutations. *Hum Mol Gen* 2010;19:2936–2946.
- Soussi T. P53 alterations in human cancer: More questions than answers. *Oncogene* 2007;26:2145–2156.
- Muller PA, Vousden KH. P53 mutations in cancer. *Nat Cell Biol* 2013;15:2–8.
- Freed-Pastor WA, Prives C. Mutant p53: One name, many proteins. *Genes Dev* 2012;26:1268–1286.
- Liu Z, Hergenbahn M, Schmeiser HH, Wogan GN, Hong A, Hollstein M. Human tumor p53 mutations are selected for in mouse embryonic fibroblasts harboring a humanized p53 gene. *Proc Natl Acad Sci USA* 2004;101:2963–2968.
- Epstein RJ. The unpluggable in pursuit of the undruggable: Tackling the dark matter of the cancer therapeutics universe. *Front Oncol* 2013;3:304.
- Toledo F, Wahl GM. MDM2 and MDM4: p53 regulators as targets in anticancer therapy. *Int J Biochem Cell Biol* 2007;39:1476–1482.
- Badal V, Menendez S, Coomber D, Lane DP. Regulation of the p14ARF promoter by DNA methylation. *Cell Cycle* 2008;7:112–119.
- Surget S, Khoury MP, Bourdon JC. Uncovering the role of p53 splice variants in human malignancy: A clinical perspective. *OncoTargets Ther* 2013;7:57–68.
- Jones M, Lal A. MicroRNAs, wild-type and mutant p53: More questions than answers. *RNA Biol* 2012;9:781–791.
- Mahmoudi S, Henriksson S, Corcoran M, Mendez-Vidal C, Wiman KG, Farnebo M. Wrap53, a natural p53 antisense transcript required for p53 induction upon DNA damage. *Mol Cell* 2009;33:462–471.
- Marcel V, Petit I, Murray-Zmijewski F, et al. Diverse p63 and p73 isoforms regulate Delta133p53 expression through modulation of the internal *TP53* promoter activity. *Cell Death Differ* 2012;19:816–826.
- Fujita K, Mondal AM, Horikawa I, et al. P53 isoforms Delta133p53 and p53beta are endogenous regulators of replicative cellular senescence. *Nat Cell Biol* 2009;11:1135–1142.
- Courtois S, Verhaegh G, North S, et al. DeltaN-p53, a natural isoform of p53 lacking the first transactivation domain, counteracts growth suppression by wild-type p53. *Oncogene* 2002;21:6722–6728.
- Slatter TL, Hung N, Campbell H, et al. Hyperproliferation, cancer, and inflammation in mice expressing a Delta133p53-like isoform. *Blood* 2011;117:5166–5177.
- Chen J, Ng SM, Chang C, et al. P53 isoform delta113p53 is a p53 target gene that antagonizes p53 apoptotic activity via BclxL activation in zebrafish. *Genes Dev* 2009;23:278–290.
- Aoubala M, Murray-Zmijewski F, Khoury MP, et al. P53 directly transactivates Delta133p53alpha, regulating cell fate outcome in response to DNA damage. *Cell Death Differ* 2011;18:248–258.
- Marcel V, Vijayakumar V, Fernandez-Cuesta L, et al. P53 regulates the transcription of its Delta133p53 isoform through specific response elements contained within the *TP53* P2 internal promoter. *Oncogene* 2010;29:2691–2700.
- Bourdon JC, Fernandes K, Murray-Zmijewski F, et al. P53 isoforms can regulate p53 transcriptional activity. *Genes Dev* 2005;19:2122–2137.
- Boldrup L, Bourdon JC, Coates PJ, Sjostrom B, Nylander K. Expression of p53 isoforms in squamous cell carcinoma of the head and neck. *Eur J Cancer* 2007;43:617–623.
- Anensen N, Oyan AM, Bourdon JC, Kalland KH, Bruserud O, Gjertsen BT. A distinct p53 protein isoform signature reflects the onset of induction chemotherapy for acute myeloid leukemia. *Clin Cancer Res* 2006;12:3985–3992.

25. Avery-Kiejda KA, Zhang XD, Adams LJ, et al. Small molecular weight variants of p53 are expressed in human melanoma cells and are induced by the DNA-damaging agent cisplatin. *Clin Cancer Res* 2008;14:1659–1668.
26. Hofstetter G, Berger A, Fiegl H, et al. Alternative splicing of p53 and p73: The novel p53 splice variant p53delta is an independent prognostic marker in ovarian cancer. *Oncogene* 2010;29:1997–2004.
27. Choy JS, Wei S, Lee JY, Tan S, Chu S, Lee TH. DNA methylation increases nucleosome compaction and rigidity. *J Am Chem Soc* 2010;132:1782–1783.
28. Huang YZ, Zhan ZY, Sun YJ, et al. Intragenic DNA methylation status down-regulates bovine IGF2 gene expression in different developmental stages. *Gene* 2014;534:356–361.
29. Maunakea AK, Chepelev I, Cui K, Zhao K. Intragenic DNA methylation modulates alternative splicing by recruiting MeCP2 to promote exon recognition. *Cell Res* 2013;23:1256–1269.
30. Tornaletti S, Pfeifer GP. Complete and tissue-independent methylation of CpG sites in the p53 gene: Implications for mutations in human cancers. *Oncogene* 1995;10:1493–1499.
31. Luo JL, Yang Q, Tong WM, Hergenbahn M, Wang ZQ, Hollstein M. Knock-in mice with a chimeric human/murine p53 gene develop normally and show wild-type p53 responses to DNA damaging agents: A new biomedical research tool. *Oncogene* 2001;20:320–328.
32. Kim SI, Hollstein M, Pfeifer GP, Besaratinia A. Unveiling the methylation status of CpG dinucleotides in the substituted segment of the human p53 knock-in (Hupki) mouse genome. *Mol Carcinog* 2010;49:999–1006.
33. Zhou H, Yong J, Sun X, et al. A human endothelial cell feeder system that efficiently supports the undifferentiated growth of mouse embryonic stem cells. *Differentiation* 2008;76:923–930.
34. Bosman A, Sartiani L, Spinelli V, et al. Molecular and functional evidence of HCN4 and caveolin-3 interaction during cardiomyocyte differentiation from human embryonic stem cells. *Stem Cells Dev* 2013;22:1717–1727.
35. Djelloul S, Fogue-Lafitte ME, Hermelin B, et al. Enterocyte differentiation is compatible with SV40 large T expression and loss of p53 function in human colonic Caco-2 cells. Status of the pRb1 and pRb2 tumor suppressor gene products. *FEBS Lett* 1997;406:234–242.
36. Ortega A, Gil A, Sanchez-Pozo A. Exogenous nucleosides modulate expression and activity of transcription factors in Caco-2 cells. *J Nutr Biochem* 2011;22:595–604.
37. Carroll AG, Voeller HJ, Sugars L, Gelmann EP. P53 oncogene mutations in three human prostate cancer cell lines. *Prostate* 1993;23:123–134.
38. Khoury MP, Marcel V, Fernandes K, Diot A, Lane DP, Bourdon JC. Detecting and quantifying p53 isoforms at mRNA level in cell lines and tissues. *Methods Mol Biol* 2013;962:1–14.
39. Rago C, Vogelstein B, Bunz F. Genetic knockouts and knockins in human somatic cells. *Nat Protoc* 2007;2:2734–2746.
40. Murray-Zmijewski F, Lane DP, Bourdon JC. P53/p63/p73 isoforms: An orchestra of isoforms to harmonise cell differentiation and response to stress. *Cell Death Differ* 2006;13:962–972.
41. Magewu AN, Jones PA. Ubiquitous and tenacious methylation of the CpG site in codon 248 of the p53 gene may explain its frequent appearance as a mutational hot spot in human cancer. *Mol Cell Biol* 1994;14:4225–4232.
42. Jjingo D, Conley AB, Yi SV, Lunyak VV, Jordan IK. On the presence and role of human gene-body DNA methylation. *Oncotarget* 2012;3:462–474.
43. Chen S, Wang DL, Liu Y, Zhao L, Sun FL. RAD6 regulates the dosage of p53 by a combination of transcriptional and posttranscriptional mechanisms. *Mol Cell Biol* 2012;32:576–587.
44. Shenker N, Flanagan JM. Intragenic DNA methylation: Implications of this epigenetic mechanism for cancer research. *British J Cancer* 2012;106:248–253.
45. Bauer AP, Leikam D, Krinner S, et al. The impact of intragenic CpG content on gene expression. *Nucleic Acids Res* 2010;38:3891–3908.
46. Pogribny I, Koturbash I, Tryndyak V, et al. Fractionated low-dose radiation exposure leads to accumulation of DNA damage and profound alterations in DNA and histone methylation in the murine thymus. *Mol Cancer Res* 2005;3:553–561.
47. Kulis M, Queiros AC, Beekman R, Martin-Subero JI. Intragenic DNA methylation in transcriptional regulation, normal differentiation and cancer. *Biochim Biophys Acta* 2013;1829:1161–1174.
48. Maunakea AK, Nagarajan RP, Bilenky M, et al. Conserved role of intragenic DNA methylation in regulating alternative promoters. *Nature* 2010;466:253–257.
49. Brennan K, Garcia-Closas M, Orr N, et al. Intragenic ATM methylation in peripheral blood DNA as a biomarker of breast cancer risk. *Cancer Res* 2012;72:2304–2313.
50. Goodman JI, Counts JL. Hypomethylation of DNA: A possible nongenotoxic mechanism underlying the role of cell proliferation in carcinogenesis. *Environ Health Perspect* 1993;101:169–172.
51. Tuck SP, Crawford L. Characterization of the human p53 gene promoter. *Mol Cell Biol* 1989;9:2163–2172.
52. Marcel V, Perrier S, Aoubala M, et al. Delta160p53 is a novel N-terminal p53 isoform encoded by Delta133p53 transcript. *FEBS Lett* 2010;584:4463–4468.

SUPPORTING INFORMATION

Additional supporting information may be found in the online version of this article at the publisher's website.